

A Review of Optical Sky Brightness and Extinction at Dome C, Antarctica

S. L. Kenyon and J. W. V. Storey

School of Physics, University of New South Wales, Sydney, NSW

suzanne@phys.unsw.edu.au

j.storey@unsw.edu.au

Accepted for publication in March 2006 issue of PASP

ABSTRACT

The recent discovery of exceptional seeing conditions at Dome C, Antarctica, raises the possibility of constructing an optical observatory there with unique capabilities. However, little is known from an astronomer's perspective about the optical sky brightness and extinction at Antarctic sites. We review the contributions to sky brightness at high-latitude sites, and calculate the amount of usable dark time at Dome C. We also explore the implications of the limited sky coverage of high-latitude sites and review optical extinction data from the South Pole. Finally, we examine the proposal of Baldry & Bland-Hawthorn (2001) to extend the amount of usable dark time through the use of polarising filters.

Subject headings: atmospheric effects — polarisation — scattering — site testing

1. Introduction

Dome C, Antarctica, is one of the most promising new sites for optical, infrared and sub-millimeter astronomy. Located at $75^{\circ}6'$ South, $123^{\circ}21'$ East and an altitude of 3250 m, Dome C is the third highest point on the Antarctica Plateau. The French (IPEV) and Italian (PNRA) Antarctic programs have operated a summertime scientific base on Dome C since 1995 (Candidi & Lori 2003). Construction of a wintertime station was completed at the beginning of 2005, leading to the first manned winter season at Dome C. Preliminary site testing has been carried out at Dome C since 1995 (Valenziano & dall'Oglio 1999; Candidi & Lori 2003) and systematic measurements of the summertime (Aristidi et al. 2005b) and wintertime (Storey et al. 2005) characteristics of the site began in 2001. The results, summarised below, indicate very favourable conditions for astronomy.

The local topography of Dome C is extremely flat, resulting in a mean ground-level wind speed of 2.9 ms^{-1} (Aristidi et al. 2005a), less than half that at most other observatories. Wintertime measure-

ments of the turbulence in the atmosphere above Dome C (with a MASS and a SODAR) indicate that, above a thin surface layer, the atmosphere is extremely stable. From above 30 metres, a median seeing of $0.27''$ is observed during the winter, with the seeing below $0.15''$ for 25% of the time (Lawrence et al. 2004). In comparison, the median seeing at the best mid-latitude sites is between 0.5 and $1.0''$. Agabi et al. (2005) measure the wintertime seeing from the ground level to be $1.9 \pm 0.5''$ and attribute this to a thin but intense layer of surface turbulence. From above this layer, which they estimate to be 36 m, the exceptionally good seeing observed by Lawrence et al. (2004) is confirmed. In addition, summertime site testing with a DIMM, i.e. while the sun is continuously above the horizon, shows a remarkable median seeing of $0.54''$ (Aristidi et al. 2005b).

The cloud cover is very low with cloud-free skies observed for at least 74% of the time (Ashley et al. 2005). In addition, the site is extremely cold and the atmosphere has very low precipitable water vapour in comparison to other sites (Valenziano & dall'Oglio 1999), leading to exceptionally low sky

TABLE 1
OBSERVABLE SKY

Site	45° zenith limit		60° zenith limit	
	Dec range	Percentage of sky	Dec range	Percentage of sky
Equator	45° S – 45° N	70 %	60° S – 60° N	86 %
Mauna Kea	26° S – 64° N	66 %	41° S – 79° N	81 %
Dome C	90° S – 30° S	25 %	90° S – 15° S	37 %
North or South Pole	90° N/S – 45° N/S	14 %	90° N/S – 30° N/S	25 %

backgrounds in the infrared (Walden et al. 2005) and the sub-millimeter (Calisse et al. 2004). Substantial improvements in atmospheric transmission are predicted at these wavelengths and a number of new spectral windows are opened up that are inaccessible at non-Antarctic sites (Lawrence 2004).

Despite these attractions, the high latitude of Dome C means that the sun spends a relatively small amount of time far below the horizon. This implies longer periods of astronomical twilight and less *optical* dark time than other sites, especially those close to the equator. Thus, although the advantages offered by Antarctica at infrared wavelengths and beyond (where sky brightness is unaffected by twilight, moonlight and aurorae) are well established (e.g. Storey et al. 2003), it remains to be seen whether the amount of usable dark time at Dome C is sufficient to allow useful advantage to be taken of the seeing conditions in the optical.

In addition to the long twilight, high latitude sites suffer from reduced sky coverage. The fraction f of the total 4π steradians of the heavens that can be seen from a site of given latitude over a 24 hour period is

$$f = 1/2(\sin N - \sin S) \quad (1)$$

where N is the northernmost declination observable and S is the southernmost. We consider two cases: a zenith limit of 45 degrees (1.4 airmasses), and a zenith limit of 60 degrees (2 airmasses). As seen in Table 1, Mauna Kea has access to 81% of the sky at 2 airmasses or less, while at Dome C only 37% of the sky is similarly available.

In the case of a high-latitude southern site such as Dome C, this restricted sky coverage is mitigated somewhat by the accessibility of several key

sources such as the Large (dec = 69° S) and Small (dec = 73° S) Magellanic Clouds and the Galactic Centre (dec = 28° S). Such southern sources are of course favourably observed from Dome C. For example, although the Galactic Centre reaches comparable maximum elevations of 44° at Dome C and 41° at Mauna Kea, it is above 30° elevation for 1300 dark hours per year at Dome C, but only 660 dark hours per year at Mauna Kea. The advantages of a high-latitude southern site for the continuous monitoring of southern objects have already been discussed by a number of authors; for example, Deeg et al. (2005).

In Section 2, we assess the amount of *usable* dark time at Dome C and examine the various contributions to optical sky brightness. The causes of atmospheric extinction are discussed in Section 3. Baldry & Bland-Hawthorn (2001) have suggested using a polarising filter to reduce twilight contributions to sky background. In Section 4 we examine the polarisation of scattered sunlight over the course of twilight to evaluate the feasibility of this idea.

2. Optical sky brightness

The night sky is never completely dark at any site. The darkest optical skies on Earth are of the order of 22.0 – 21.1 V mag arcsec⁻² at zenith (Leinert et al. 1998). See Leinert et al. (1998) for a comprehensive discussion of diffuse night sky brightness, Patat (2003) for an in depth survey of *UBVRI* night sky brightness at ESO-Paranal, and Benn & Ellison (1998) for a review of sky brightness measurements at La Palma.

On a moonless night, long after the sun has set, the sky is brightened by aurorae, airglow, zo-

TABLE 2
CONTRIBUTIONS TO THE LIGHT OF THE NIGHT SKY

Source	Function of	Physical Origin
Scattered sunlight	Ecliptic coordinates, season, location, aerosols	Sunlight scattering from molecules and particles in the upper atmosphere
Moonlight	Lunar phase, position of the moon, aerosols	Sunlight reflected from the lunar surface, then scattered in the atmosphere
Aurora	Magnetic latitude, season, magnetic activity, solar activity,	Excitation of upper atmosphere atoms and molecules by energetic particles
Airglow	Zenith angle, local time, latitude, season, solar activity, altitude, geomagnetic latitude	Chemiluminescence of upper atmosphere atoms and molecules
Zodiacal light	Ecliptic coordinates	Sunlight scattered by interplanetary dust
Integrated starlight	Galactic coordinates	Unresolved stars in the Milky Way
Diffuse galactic light	Galactic coordinates	Scattering of starlight by interstellar dust
Integrated cosmic light	Galactic coordinates, cosmological red shift	The universe
Light pollution	Proximity to civilisation	Artificial lighting

NOTE.—From Roach & Gordon (1973)

diacal light, integrated starlight, diffuse galactic light, extra-galactic light and artificial sources (see Table 2). As first noted by Rayleigh (1928) the sky brightness at a particular site varies with solar activity; for example, Walker (1988) records a change of at least 1 mag arcsec⁻² in sky brightness with solar activity. Atmospheric scattering of the flux from each of these sources adds significantly to the sky brightness; for example, the contribution from zodiacal light can be increased by more than 15% by scattering and that from integrated starlight by 10 – 30% (Leinert et al. 1998). During twilight, the scattered sunlight usually makes the dominant contribution to the overall sky brightness, while the flux from direct and scattered moonlight adds a further strong contribution when the moon is above the horizon. The best dark conditions occur at a site with minimal atmospheric scattering.

In this section we discuss each source of sky brightness at Dome C and provide a comparison to Mauna Kea, Hawaii, which we select because it is the closest major observatory to the equator.

2.1. Scattered sunlight and usable dark time

Sunlight is the strongest contributor to the brightness of the sky. During the day the surface of the Earth is illuminated by *direct* sunlight and sunlight *scattered* by atmospheric molecules and particles. After sunset, the surface of the Earth is only illuminated by scattered sunlight; the direct component illuminates the atmosphere above the level of the Earth’s shadow. Over the course of twilight the scattered sunlight contribution to sky brightness decreases, as higher and less dense levels of the atmosphere are illuminated (Rozenberg 1966). In the absence of moonlight and artificial sources, scattered sunlight completely dominates the sky brightness until the sun reaches a zenith angle of about 98 degrees (Pavlov et al. 1995). The relative contribution of scattered sunlight to total sky brightness then decreases sharply to a negligible level, and nighttime starts. In the V-band this occurs when the sun is depressed 17 – 19° below the horizon; if there is a high amount of scattering in the atmosphere this can be extended to depressions of 20 – 23° (Rozenberg 1966). Astronomical

nighttime is usually considered to begin when the sun is more than 18° below the horizon.

For solar zenith angles greater than about 98° , multiple scattering accounts for essentially all of the sunlight contribution to sky brightness; this contribution is affected by the aerosol content in the atmosphere (Pavlov et al. 1995; Ugolnikov et al. 2004). Dome C has an exceptionally clear atmosphere with no dust, haze, smog or sand aerosols (see Section 3 for a discussion on scattering at Dome C) and therefore it is expected that the intensity of multiply scattered light will be at a minimum possible level. Paradoxically, the lack of aerosols will, however, decrease the attenuation of sunlight that grazes the earth, with the result that at mid-twilight the intensity just above the earth’s shadow could be brighter at some wavelengths than at sites with less clear skies. This has the effect of lowering the effective altitude of the so-called “twilight layer” (Ugolnikov 1999; Ugolnikov & Maslov 2003), creating an opportunity for enhanced scattering by the denser gas at those lower altitudes. A further effect that could brighten the Dome C sky is the high albedo of the snow that covers the Antarctic plateau, which will increase the sky brightness by a small amount at sunset. However this effect decreases with increasing solar zenith angles and is negligible once the sun has set (Anderson & Lloyd 1990). During periods when the moon is above the horizon, the high albedo of the snow may also increase the sky brightness beyond that normally experienced during grey time.

From the above discussion, it is clear that the twilight sky brightness at Dome C and the solar depression angle at which nighttime commences cannot be calculated in a straightforward manner. Both parameters can only be quantified by direct measurement or by detailed modelling using accurate atmospheric aerosol profiles.

Using the formal definition above, Dome C has less astronomical nighttime than lower latitude sites, with long periods of twilight. From a simple geometric calculation, Dome C has about 50% of the astronomical nighttime of Mauna Kea, as shown in Figure 1. The cloudiness of each site also needs to be taken into consideration when looking at the amount of dark time available for optical observations. On the basis of 2001 data, Ashley et al. (2005) report the skies at Dome C to be

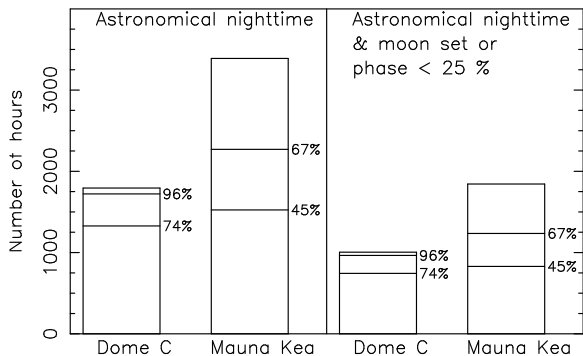


Fig. 1.— Comparison of the available dark time and cloud statistics (see text) at Dome C and Mauna Kea. The left panel shows the number of hours of formal astronomical nighttime (i.e. when the sun is further than 18° below the horizon). The right panel shows the number of hours of astronomical nighttime when the moon is below the horizon or less than one quarter phase. The percentage bars indicate the usable dark time once cloud cover is taken into account.

cloud-less for 74% of the time, with the remaining 26% having more than $1/8$ cloud cover. While this is a tentative conclusion based on less than a full year of data from Dome C, new independent measurements in 2005 (Aristidi et al. 2005c) suggest that the percentage of cloud-free skies at Dome C may be as high as 96%. In comparison (Ortolani 2003 and references therein) report 45% photometric nights (no clouds) and 67% spectroscopic nights ($1/4 - 1/10$ cloud cover) at Mauna Kea. These percentages are also displayed in Figure 1.

If the more optimistic figure of Aristidi et al. (2005c) is confirmed, Dome C will be seen to have a comparable number of usable, astronomically dark hours to Mauna Kea.

2.2. Moonlight

The sky brightness contribution caused by the Moon depends on its position and phase. Moonlight illuminates the surface of the Earth both directly and by scattering, in a similar fashion to sunlight. Figure 2 shows the elevation of the sun (contour lines) and moon (gray scale shading), together with the phase of the moon, for Dome C and Mauna Kea over the course of one year (2005).

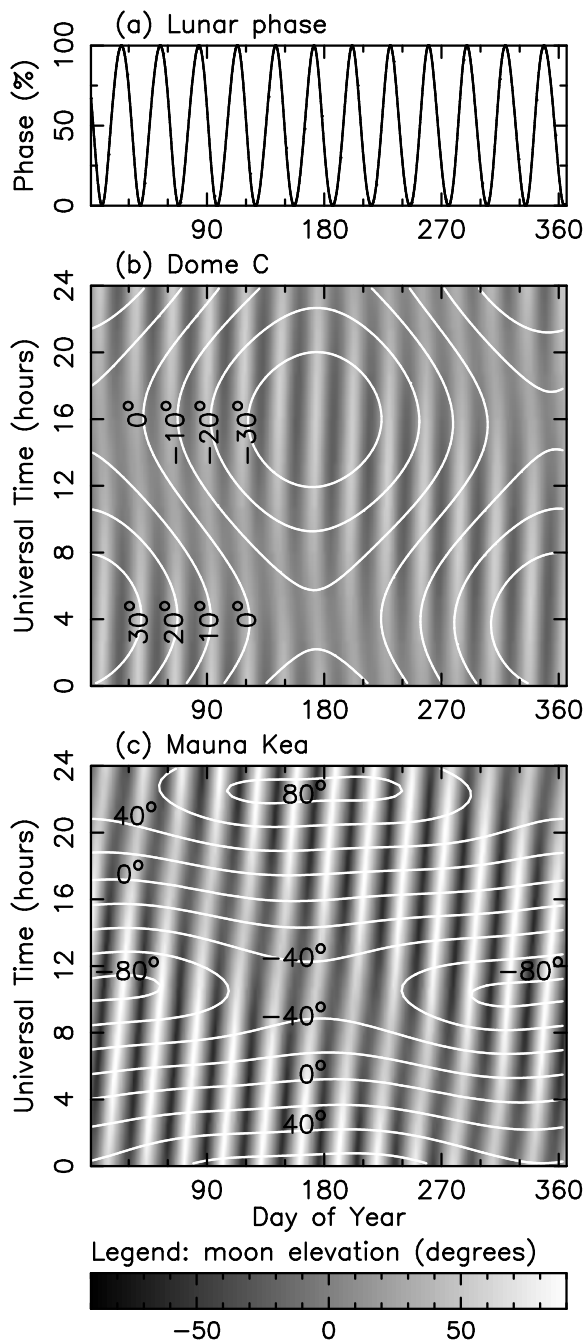


Fig. 2.— Lunar phase (a), and solar and lunar elevation angles at Dome C (b) and Mauna Kea (c) over the course of one year (2005). In plots (b) and (c) the contours show the solar elevation angles and the grey scale shows the lunar elevation angles according to the scale below.

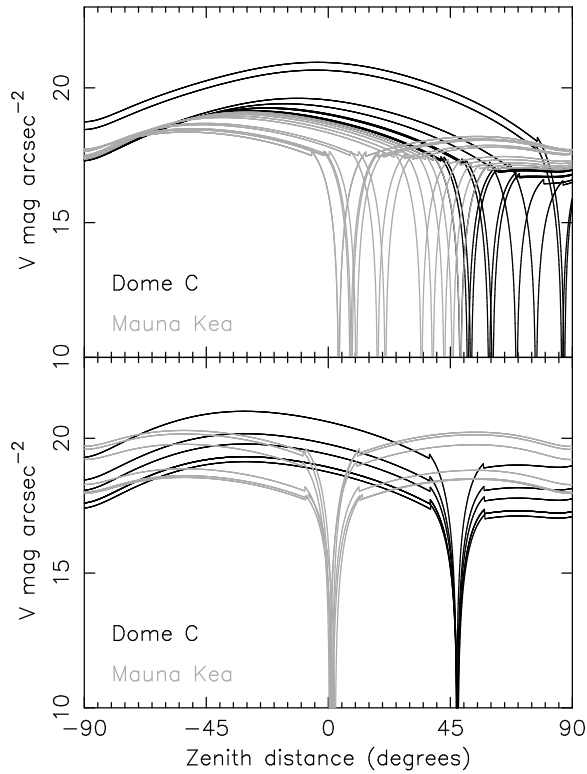


Fig. 3.— Top panel: Scattered moonlight brightness as a function of zenith angle when the *full* moon reaches its highest altitude in each month (in 2005). Bottom panel: Scattered moonlight contribution for the highest altitude of the moon in each month, regardless of phase. Each plot shows the moonlight contribution for a cross section of the sky that passes through the moon and the zenith, for Dome C (black) and Mauna Kea (grey), and each curve represents a different month.

The darkest skies are when the sun is far below the horizon and either the moon is below the horizon (dark shading) or the phase of the moon is close to new. The 18.6 year lunar nodal cycle changes the declination range of the moon; this ranges between $\pm 29^\circ$ and $\pm 18^\circ$. At Dome C the moon reaches a maximum elevation between $\sim 33^\circ$ and $\sim 43^\circ$ depending on this cycle; at Mauna Kea the moon can pass through the zenith, independent of nodal cycle.

To quantify the effect of the different range of moon elevation at Dome C and Mauna Kea, we calculated the moonlight brightness using the model of Krisciunas & Schaefer (1991). The lunar

phase (from full moon to new moon and back) cycles over one month; for each month in 2005 we calculated the sky brightness when (1) the *full* moon was at the highest elevation for that month and (2) the moon was at the highest altitude, regardless of phase. A cross section of the sky, cutting through the position of the moon and the zenith at those times, is plotted in Figure 3. In the calculation we set the extinction coefficient for both sites to the median value for Mauna Kea (0.12 mag/airmass at 550 nm).

The full-moon contribution at Dome C is less than that at Mauna Kea by several magnitudes at zenith, with little difference at the horizon. For the second case, excluding the sky close to the moon, the contribution is once again less at Dome C than at Mauna Kea. As at all sites, this contribution reaches a minimum between 60° and 90° away from the moon (Patat 2004). This advantage to Dome C is reduced to some extent by the fact that the fullness of the moon and its maximum elevation are highly correlated at Dome C (as seen in Figure 2) but only weakly so at Mauna Kea. Skies that would otherwise be dark are brightened at zenith by moonlight by a median value of $1.7 \text{ V mag arcsec}^{-2}$ at Dome C and $2.1 \text{ V mag arcsec}^{-2}$ at Mauna Kea, averaged over the epoch 2005 – 2015.

2.3. Aurorae

Aurorae are the spectacular lights seen dancing across the skies in (mainly) polar regions. As highly energetic particles from the sun travel into the atmosphere they collide with upper atmosphere atoms and molecules, exciting them to higher energy levels. The excited atoms and molecules then decay radiatively. Aurorae are generally (though not exclusively) confined to an annular region $15 - 25$ degrees from the *geomagnetic* poles (see Figure 4) and have a strong dependence on the 11 year solar sunspot cycle. The geomagnetic poles are the two positions where the Earth’s theoretical magnetic dipole intersects the Earth’s surface. The positions of the geomagnetic poles move around, and in January 2005 the geomagnetic south pole was at a geographic position of 79.3° S , 108.5° E (NGDC 2005). The size and position of the auroral oval changes with solar activity; see OVATION (2005) for plots of the size and position of the auroral oval from December

1983 to the present. Aurorae typically occur $100 - 250 \text{ km}$ above the ground but can occur at altitudes anywhere between 80 and 1000 km . In the V-band the strongest auroral emission is from neutral oxygen at 557.7 nm . Aurorae can vary rapidly in intensity and position across the sky. Dome C lies about 10° away from the inner edge of the typical auroral oval, so little auroral activity is expected. In comparison, South Pole is located very close to the inner edge of the auroral oval and experiences considerable auroral activity. The position of Dome C relative to the auroral oval means that most auroral activity will be close to the horizon as well as low in intensity. Figure 4 shows the geographic positions of Dome C, South Pole (geographic), the typical auroral oval and the geomagnetic south pole. Using simple geometry we calculated the sky position at Dome C for aurorae occurring at 100 and 250 km altitude in the auroral oval, as a function of angular separation between Dome C and the aurora. Aurorae at 100 km altitude will usually be below the horizon at Dome C; at 250 km altitude this occurs at 16° separation. The dotted circle in Figure 4 shows this range. The results of the calculations are shown in Table 3. The first column is the angular separation between the aurora and Dome C, D is the distance in kilometres from Dome C to the aurora, and E is the elevation angle of the aurora at Dome C. The elevation angle of typical aurorae seen from Dome C will be between the horizon and 7° elevation, and they will be between 1160 and 2000 km away. Sun-aligned quiet arcs will not decrease with increasing magnetic latitude in the same fashion as normal aurorae, however they are significantly less intense than the aurorae occurring within the auroral oval (Gary Burns, 2005, private communication).

Dempsey et al. (2005) used satellite measurements of the electron flux above Dome C to calculate the expected intensity of aurorae. They found that in the V band the intensity of the auroral contribution to sky background was less than $22.7 \text{ mag arcsec}^{-2}$ for 50% of the wintertime during a solar maximum year and below $23.5 \text{ mag arcsec}^{-2}$ during solar minimum.

Aurorae are therefore expected to have a minor impact on optical astronomy at Dome C, even without the use of narrow-band filters to remove the brightest emission lines. The contribution to

TABLE 3
POSITION OF AURORAE AT DOME C

Angular separation	Aurora altitude: 100 km		Aurora altitude: 250 km	
	D (km)	E	D (km)	E
10°	1125	0°	1161	7°
11°	1236	-1°	1271	6°
12°	1347	-2°	1382	4°
13°	1459	-3°	1493	3°
14°	1570	-3°	1604	2°
15°	1681	-4°	1716	1°
16°	1792	-5°	1827	0°
17°	1903	-6°	1938	-1°

NOTE.—The first column is the angular separation between the aurora and Dome C. From this we derive the distance, D , from the Dome C to the aurora and the elevation angle, E , of the aurora at Dome C.

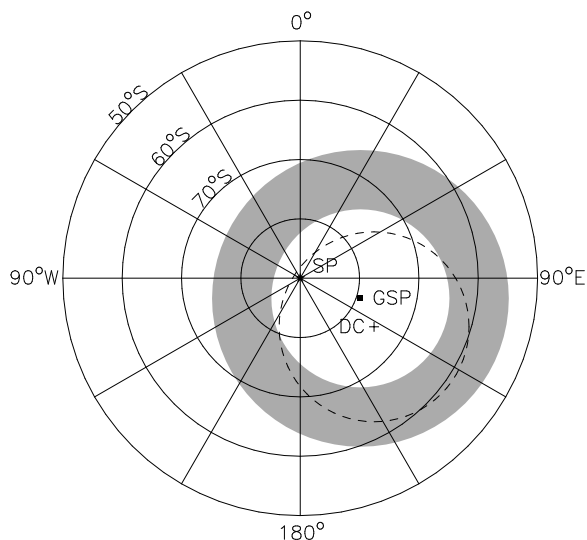


Fig. 4.— Schematic of the typical southern auroral oval, showing the geographic South Pole (SP), Dome C (DC) and the geomagnetic south pole (GSP). The auroral oval, shown in grey shading, is typically located 15 – 25° from the geomagnetic south pole (GSP). Aurorae at 250 km altitude will be above the horizon at Dome C only if they lie within the dotted line.

sky brightness at Mauna Kea by aurorae is of course negligible.

2.4. Zodiacal light

Zodiacal light is caused by sunlight scattering from the diffuse cloud of interplanetary dust that lies largely in the plane of the solar system. Zodiacal light is strongest near the sun and is generally seen as a cone of light with its base at the horizon, decreasing in intensity towards the zenith, with another maximum sometimes seen at the anti-solar point. The intensity is dependent on wavelength, observer position and sky position. Zodiacal light is polarised, reaching a maximum polarisation of about 20% (Leinert et al. 1998).

The zodiacal contribution to sky brightness at Dome C and Mauna Kea was calculated over one year, using the method described by Leinert et al. (1998). All correction factors in the model were set to unity; thus there is a possible variation in flux of up to 30%. Calculations were limited to astronomical nighttime. Two sky positions were looked at: the zenith, and a zenith distance of 60° at the same azimuthal position as the sun. The results are shown in Figure 5.

In the V-band, the zenith brightness of zodiacal light at Dome C is always *darker* than 23.1 mag arcsec⁻² because the zodiac is always fairly low on

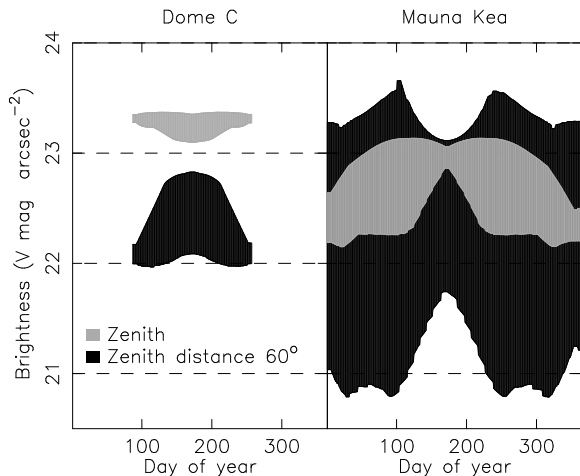


Fig. 5.— The range of zodiacal contribution to sky brightness (V mag arcsec $^{-2}$) at Dome C (left) and Mauna Kea (right), over 1 year, for sun elevations less than -18° . The grey shading is for observations at zenith and the black is for a zenith distance of 60° at the same azimuthal position as the sun.

the horizon. In comparison, at Mauna Kea the zodiacal sky brightness at zenith is always *brighter* than about 23.1 mag arcsec $^{-2}$, reaching a maximum contribution of about 22.1 mag arcsec $^{-2}$. At a zenith distance of 60° and in the azimuthal direction of the sun, the zodiacal light at Dome C is always darker than about 22 mag arcsec $^{-2}$; at Mauna Kea it can get as bright as about 20.8 mag arcsec $^{-2}$. This reduced contribution from zodiacal light is of course not a characteristic of the site per se, but rather a reflection of the fact that a different part of the sky passes overhead at Dome C than does at Mauna Kea.

2.5. Airglow

Airglow, at night, is the chemiluminescence of upper atmosphere molecules and atoms. This so-called “nightglow” includes a quasi-continuum from NO_2 and a number of discrete emission lines, the strongest by far being from the hydroxyl radical. A number of visible nightglow emission lines are listed in Table 4, along with the typical altitude of the emitting atmospheric layer and typical intensities.

Nightglow is unpolarised and on a large scale increases from zenith to the horizon, as described

by the van Rhijn function. On a small spatial scale nightglow emissions are uneven and blotchy across the sky. Nightglow emissions vary over short and long time scales.

Nightglow emissions are mainly from the thin mesospheric layer, centred at an altitude of $85 - 90$ km. OH Meinel bands are primarily excited by a reaction between ozone and atomic hydrogen (Le Texier et al. 1987). The concentrations of O_3 and H depend on the atomic oxygen mixing ratio (Le Texier et al. 1987) which is largely controlled by the transport processes in the mesosphere and lower thermosphere (Garcia & Solomon 1985). At low and mid-latitudes there is a semi-annual variation in atomic hydrogen and hence OH nightglow (Le Texier et al. 1987).

Because of the efficient mechanisms that transport reactants from sunlit locations to the poles, there is no reason to expect a diminution in the chemiluminescence of species such as OH and O_2 during the long polar night. Phillips et al. (1999) observed a small reduction in OH emission at South Pole in 1995 relative to temperate sites, but this is more likely explained by the known highly variable nature of OH emission. Continuous monitoring of the Meinel bands of OH in J band with a Michelson interferometer has been carried out at the Pole since January 1992, and the data are now publicly available (Sivjee et al. 2005). As expected, these data show very large hourly and nightly variations, with no diminution in average intensity as the winter progresses.

Zaragoza et al. (2001) measured the OH nightglow emissions in a narrow spectral band near $4.6 \mu\text{m}$ for just under one year. Using the Improved Stratospheric and Mesospheric Sounder on the UARS satellite they have almost full global coverage (80° N to 80° S). They find at high latitudes a springtime minimum in the OH emission $\sim 30\%$ below the global mean, although this is only for one year of data. During the Northern hemisphere winter solstice period their averaged measured intensities of OH nightglow at high latitudes and mid-latitudes are the same to within the errors.

Measurements of OH nightglow between 837.5 and 856.0 nm at Davis, Antarctica ($68^\circ 35'$ S, $77^\circ 58'$ E) over 7 years (Burns et al. 2002), show a barely significant seasonal variation in emission intensity, although there are large day-to-day vari-

TABLE 4
AIRGLOW EMISSIONS AT ZENITH IN THE VISIBLE RANGE

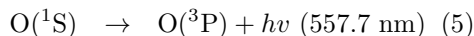
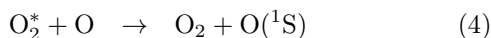
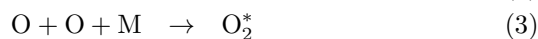
Source	Wavelength (nm)	Height (km)	Typical intensity (R)	Comments
Nightglow from chemical association				
O ₂	260 – 380	90	0.5R/Å	Herzberg bands
OH	600 – 4500	85	4.5 MR	Strongest bands in NIR
NO ₂	500 – 650	90	250	Nightglow continuum
O I	557.7	95	250	
Na D	589.0, 589.6	~ 92	50	Strong seasonal variation
O ₂	761.9	~ 80	1000	Atmospheric bands
O ₂	864.5	~ 80	1000	Atmospheric bands
Nightglow from ionic reactions				
N	519.8, 520.1	1		
O I	557.7	250 – 300	20	High atmospheric, chiefly in tropics during enhancement of OI 630.0,636.4
O I	630.0	250 – 300	100	Sporadic enhancements in tropics
O I	636.4	250 – 300	20	assoc. with ionospheric disturbances

References. — Roach & Gordon (1973), Leinert et al. (1998) and references therein

NOTE.—1R= $1/4\pi \times 10^{10}$ photons m⁻² s⁻¹ steradian⁻¹

ations (Gary Burns & John French, 2005, private communication). We therefore expect that the sky brightness in those bands (650 nm – 2.2 μ m) dominated by OH emission will be essentially identical at Dome C to that at all other observatory sites, including Mauna Kea.

The strongest nightglow emission in the visible is the 557.7 nm line of O(¹S). As discussed in Shepherd et al. (1997), the 557.7 nm emission is caused by the following reactions:



where M is usually N₂. O₂^{*} and O(¹S) have very short lifetimes, however atomic oxygen above 100 km altitude has a long lifetime and can be transported globally before recombination.

Using a model of global tides in the thermosphere, ionosphere and mesosphere, Yee et al. (1997) predict an *increase* of some 50% in the O(¹S) 557.7 nm emissions towards the poles, although more data are needed to confirm this model. Note, however, that this single strong line can be easily filtered from astronomical measurements. In general, we expect that there will be little difference in overall airglow emissions between Antarctic and temperate sites.

2.6. Integrated starlight, diffuse galactic light and integrated cosmic light

Telescopes can only identify, as individual objects, those stars that are brighter than a certain magnitude. The integrated flux from all stars fainter than this magnitude contributes to the sky background. The limiting magnitude of a telescope depends on the *seeing* of the site, the atmospheric extinction and the size of the telescope. The expected excellent seeing and low atmospheric extinction at Dome C will ensure that the limiting magnitude of even a small telescope will be sufficient to reduce the integrated unresolved starlight to negligible levels.

Diffuse galactic light is a result of scattering of starlight by interstellar dust and is brightest in the Milky Way where the concentrations of stars and dust are highest. The typical zenith value of diffuse galactic light in the V band is about 23.6 mag

arcsec⁻² (Roach & Gordon 1973). At Dome C the galactic plane continuously circles close to the zenith, leading to a relatively high contribution from integrated starlight and diffuse galactic light compared to other sites. At Dome C the galactic latitude of the zenith ranges between –10° to –40°, whereas at Mauna Kea the range is much larger: –40° to +85° with the galactic plane close to the horizon for some of the time.

The integrated cosmic light (redshifted starlight from unresolved galaxies) contribution, at all sites, is very small in comparison to all other sources of sky brightness. No firm measurement exists for its value, however upper and lower limits have been measured and estimated from models, giving a range of about 25 to 30 mag arcsec⁻² at 550 nm (Leinert et al. 1998 and references therein).

Dome C will receive a comparatively higher contribution of light from the galactic plane than lower latitude sites. However this contribution is small when compared to other sources of sky brightness and, as with zodiacal light, depends on the sky position being observed.

2.7. Light Pollution

Light pollution from towns and cities can cause a considerable increase in the brightness of the night sky. Light pollution is mostly caused by light from vapour lamps (Hg-Na emission lines in blue-visible) and incandescent lamps (weak continuum) (Benn & Ellison 1998 and references therein). Garstang (1989a) modelled the increase of the zenith sky brightness caused by light pollution at various sites. Garstang (1989b) further predicts the increase in light pollution at various sites over time. For example, Garstang (1989b) predicts the artificial sky brightness will increase the total sky brightness by between 0.04 and 0.53 mag arcsec⁻² at Mauna Kea by the year 2020. This estimate is based on projections of population increase and does not take into account changes in light sources and systems or unforeseen circumstances such as major tourist or housing developments nearby the sites, as noted in the paper. Light pollution can significantly increase the brightness of the night sky. For further discussions of night sky brightness modelling and world maps of the artificial sky brightness see Cinzano & Elvidge (2001, 2004) and references within.

The closest station to Dome C (Vostok at 78°27'51''S 106°51'57'' E) is 560 km away. The placement of external lighting at the Dome C station itself will be carefully considered in relation to astronomical observations. With proper planning there should continue to be no artificial light pollution at Dome C, while the light pollution at other sites is likely to increase.

3. Atmospheric Extinction

Atmospheric extinction is caused by the scattering and absorption of light as it travels through the atmosphere. Extinction in the atmosphere decreases the amount of light received by an observer and lowers the limiting magnitude of a telescope.

As radiation travels from the top of the atmosphere to the surface of the Earth it may be transmitted directly to the surface with no attenuation or scattering. Alternatively, it may undergo one or more of the following processes: single or multiple scattering, reflection from the Earth's surface, and absorption by an atmospheric particle or molecule. Scattering is described by Rayleigh scattering ($2\pi r \ll \lambda$) from gaseous molecules, Mie scattering ($2\pi r \sim \lambda$) from aerosol particles (where r is the radius of the particle and λ is the wavelength of the light interacting with the particle), and a small amount of scattering due to turbulent cells. Radiation is absorbed in the atmosphere by molecules (especially water vapour and ozone), aerosol particles and liquid or frozen water in clouds (Coulson 1988). All these processes of scattering and absorption are strong functions of altitude and wavelength and their effect, except for Rayleigh scattering, is highly variable with location and time.

Scattering has two effects on astronomical observations: it increases the overall sky brightness and decreases the flux received from the object being observed. Atmospheric absorption will also decrease the signal flux. Beer's law describes the attenuation of light caused by the atmosphere:

$$I_\lambda = I_0 \exp(-\tau_\lambda^R - \tau_\lambda^A - \tau_\lambda^W - \tau_\lambda^O - \tau_\lambda^C) \quad (6)$$

where I_λ is the flux received by the observer, I_0 is the flux outside the atmosphere and τ is the wavelength-dependent optical thickness of the atmosphere; a sum of the Rayleigh R , aerosol A , water vapour W , ozone O and cloud C optical

thicknesses.

3.1. Rayleigh Optical Depth

Rayleigh optical depth is dependent on the molecular composition of the atmosphere and is proportional to λ^{-4} . The molecular composition varies with the pressure, temperature and refractive index of the atmosphere above the Earth's surface. Rayleigh optical depth is essentially constant between sites of similar elevation. See Bodhaine et al. (1999) and Tomasi et al. (2005) for further details on Rayleigh optical depth calculations.

3.2. Aerosol optical depth

Aerosol optical depth is extremely variable with geography and time and is dependent on the concentration, size, refractive index and chemical composition of the aerosol particles. The complex refractive index of a particle is $m = n - ik$, where n is the real part (1.45 – 1.60) and k (0.001 – 0.1) the imaginary part; the bracketed ranges are typical values for most “dry” atmospheric aerosols (Coulson 1988). High humidity in the air can cause condensation to occur on aerosol particles, which changes the index of refraction, size and mean density of the particle. The vertical profile of the aerosol content of the atmosphere can be derived from intensity measurements during twilight as different levels of the atmosphere are illuminated by sunlight. For the best sites the aerosol optical depth needs to be as small as possible.

No aerosol measurements have been taken yet at Dome C; however aerosol measurements at South Pole and Mauna Loa, Hawaii, have been taken since 1974 (Bodhaine (1995) and references therein). The wavelength-dependent aerosol scattering coefficient is defined as $\beta_s = N_s \sigma_s$, where N_s is the number concentration of aerosol particles and σ_s is the scattering cross section. At the South Pole $\beta_s(550 \text{ nm})$ is very low, varying between $(1 - 4) \times 10^{-7} \text{ m}^{-1}$. The maximum values are seen in winter and are associated with long-range mid-tropospheric transport of sea salt from the coast. Scattering from polar stratospheric clouds may also contribute to the maximum seen in winter (Collins et al. 1993). In comparison, at Mauna Loa, $\beta_s(550 \text{ nm})$ varies between $(6 - 60) \times 10^{-7} \text{ m}^{-1}$, showing maximum values during winter and

spring, associated with dust transport.

3.3. Absorption optical depths

The absorption of visible and IR radiation in the atmosphere is dependent on pressure, temperature and the absorbing gas (largely water vapour, ozone) and aerosol concentrations; all of which vary with location, height and time (Zuev 1974). Atmospheric absorption is described by the imaginary part k of the refractive index of the atmospheric particles, such that the absorption coefficient (m^{-1}) is

$$\beta_{ap} = \frac{4\pi k}{\lambda} = \sigma_a N_a \quad (7)$$

where σ_a is the absorption cross section (m^2) and N_a is the concentration of absorbers (m^{-3}). At most wavelengths water vapour is the primary absorber in the atmosphere and its concentration is highly variable. The optical thicknesses for water vapour and clouds show complicated and highly variable changes in magnitude with wavelength and time. The aerosol absorption coefficient for light at 550 nm at South Pole varies between 2×10^{-10} and $5 \times 10^{-7} \text{ m}^{-1}$, comparatively lower than at Mauna Loa (from 1×10^{-8} to $3 \times 10^{-7} \text{ m}^{-1}$) (Bodhaine 1995 and references therein).

To minimise the total optical depth, a site with low water vapour concentration, few clouds and low aerosol concentration is required. Dome C fits all these criteria, and may have an even lower atmospheric aerosol content than South Pole because of its greater distance from the coast. We therefore expect both the scattering and absorption by aerosols to be typically an order of magnitude less at Dome C than at Mauna Kea, and that the overall atmospheric extinction will be the minimum possible.

At ultraviolet wavelengths, the reduced atmospheric aerosol content should lead to improved transmission. However, the infamous ‘‘ozone hole’’ is unlikely to be of significant benefit to astronomers. From January until August the column density of ozone in the atmosphere above the South Pole is typically the same as at other sites around the world. It is only during the spring months that the ozone content falls to as low as 40% of its normal value. Unfortunately, these low ozone values do not occur in the dark winter months. Furthermore, because the Hartley bands

of ozone are heavily saturated, even a reduction in ozone column density by a factor of three (i.e., somewhat greater than is actually observed over the South Pole) would shift the UV cutoff wavelength of the atmosphere by only about 5 nm.

4. Using a polariser during twilight

Dome C experiences long periods of twilight, where the solar depression angle is between zero and -18° . Baldry & Bland-Hawthorn (2001) have suggested using a polarising filter to reduce the scattered sunlight contribution to sky brightness during twilight, to achieve ‘‘dark time’’ observing. At sites close to the equator this probably would not be worthwhile because twilight only lasts a few hours. However, the use of a filter during twilight in Antarctica could be very beneficial, as noted in that paper. For example, if dark time conditions at Dome C could be achieved at a solar depression angle of 15° , the available ‘‘dark’’ observing time would increase by 18%.

In the next section we discuss the intensity and polarisation of twilight and in Section 4.2 we review the idea of Baldry & Bland-Hawthorn (2001). In Section 4.3 we look at measurements of the polarisation of *daylight* at South Pole. In section 4.4 we look in some detail at measurements of the total polarisation of *twilight* in the atmosphere as a function of solar zenith angle Z_\odot and wavelength λ , and explore the benefit that might be gained by using a polariser on an Antarctic telescope.

4.1. Intensity and polarisation of twilight

During twilight, the total background light I_B reaching the surface consists of singly scattered sunlight I_S , multiply scattered sunlight I_M , and the night sky illuminance I_N .

$$I_B = I_S + I_M + I_N \quad (8)$$

The night sky illuminance includes all the sources of sky brightness discussed in section 2, except moonlight and sunlight. Sunlight becomes polarised in the atmosphere through scattering interactions with permanent atmospheric gases, variable gases and solid and liquid particles suspended in the atmosphere. The total degree of polarisation of twilight is given by:

$$P = \frac{I_S}{I_B} P_S + \frac{I_M}{I_B} P_M \quad (9)$$

where P_S and P_M are the degrees of polarisation of singly and multiply scattered light. The polarised component of the background night sky flux is assumed to be negligible with respect to that of the scattered sunlight.

Singly scattered sunlight is a combination of sunlight scattered from molecules and from aerosols. The polarisation of sunlight singly scattered from molecules can be modelled (see Coulson 1988); in this model, the atmosphere is considered to contain only permanent gases with no aerosols, clouds, water vapour or ionised particles; the scattering particles are assumed to be spherical; and the refractive index very close to unity.

Figure 6 shows the results of a calculation using this model for $Z_\odot = 90^\circ, 96^\circ, 102^\circ$ and 108° (i.e. from sunset to the end of astronomical twilight). The light shading shows that a large section of the singly scattered sunlight perpendicular to the sun is polarised to a high degree, whereas in the direction parallel to the sun the polarisation rapidly drops off with zenith angle. In the lower panel of the figure the polarisation at zenith as a function of increasing solar zenith angle is shown for $P_S^{\text{MAX}} = 85$ and 100%. This indicates that singly scattered light (in an ideal atmosphere) is highly polarised over a substantial fraction of the sky during twilight.

The degree of polarisation (although not the pattern) in the real atmosphere differs from this model because of non-isotropic molecular scattering, aerosol scattering and reflection from the Earth’s surface.

Multiply scattered sunlight is polarised to a lesser degree than singly scattered light. Multiple scattering is confined to a thin atmospheric layer that is much closer to the Earth’s surface than the single scattering layer (Ougolnikov 1999). The polarisation of sunlight can be further reduced by reflection from high level clouds and cloud-forming particles, e.g. Pomozi et al. (2001).

The highest polarisation of light occurs when water vapour and aerosol concentrations are very low and the Rayleigh optical depth is as small as possible, suggesting that scattered sunlight at Dome C should, in general, be more highly polarised than at temperate or tropical sites.

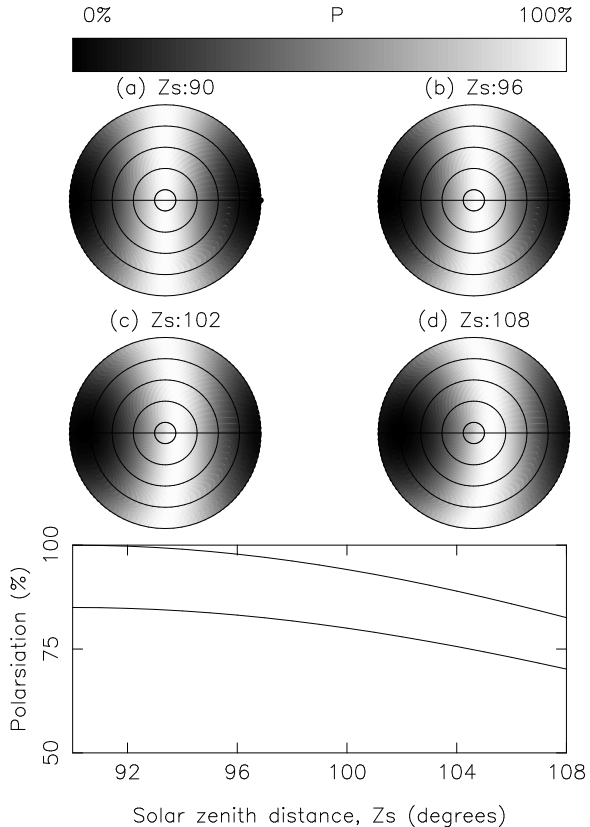


Fig. 6.— Top: Full sky plots of the degree of polarisation using the Rayleigh model for sun zenith angles of (a) 90° , (b) 96° , (c) 102° and (d) 108° (i.e. from sunset to the end of astronomical twilight). The circles indicate elevation angle and are spaced 20° apart. Bottom: Polarisation at zenith as a function of solar zenith angle for a Rayleigh atmosphere with assumed maximum polarisation of 100% and 85%.

4.2. Potential improvements with a polariser

Using an appropriately oriented polariser will reduce the sky background to:

$$I'_B = \tau I_B [1 - P(1 + 2\gamma)] \quad (10)$$

where τ is the transmission of the polariser with unpolarised light and γ is the extinction of the polariser (Baldry & Bland-Hawthorn 2001).

Assuming photon-noise-limited observations, a perfect polariser and no change in instrument response with polarisation, a polariser will be bene-

ficial whenever

$$P \gtrsim (1 - \tau) \frac{I_O + I_B}{I_B} \quad (11)$$

where I_O is the magnitude of the object. Objects that are very dark compared to the sky background require $P > 52\%$ for $\tau = 0.48$; for a sky background of $20.5 \text{ mag arcsec}^{-2}$ and object of magnitude of $22 \text{ mag arcsec}^{-2}$, the polarisation must be greater than 65% for the use of a polariser to be beneficial.

Baldry & Bland-Hawthorn (2001) assume the polarisation of twilight is always 85% , independent of solar elevation angle. Although the polarisation of singly scattered light is probably always above 85% (for a clear atmosphere), the total polarisation depends on the relative intensity of the singly and multiply scattered light to the total sky intensity, as in Equation 9.

4.3. Polarisation at the South Pole and effects of ice precipitation

At this stage no measurements of the polarisation of twilight at Dome C have been taken. However, Fitch & Coulson (1983) measured the polarisation of the sky at the South Pole, during summer, under clear sky conditions, and when ice crystals were evident. They found the degree of polarisation to be very high, under clear sky conditions, and close to the results given by a Rayleigh model. The presence of ice crystals reduced the degree of polarisation and caused a greater effect at longer wavelengths. We expect that the atmosphere at Dome C will also closely resemble a Rayleigh atmosphere and therefore, at small solar depression angles the scattered light will be highly polarised.

4.4. Spectral characteristics of polarisation as a function of solar depression angle

Over the course of twilight the polarisation and intensity of skylight changes as different levels of the atmosphere are illuminated.

In this section we look at measurements of the twilight polarisation and intensity at various high altitude, clean sites. The behaviour of the total degree of polarisation P as a function of solar zenith angle Z_\odot can be roughly divided into three regimes; we assess the benefit of using a polariser

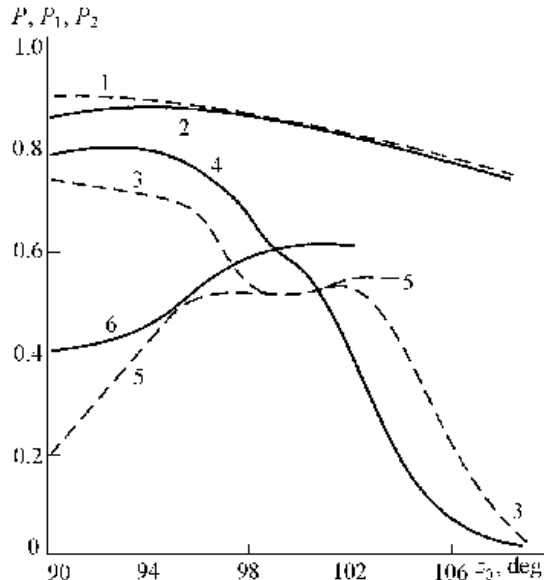


Fig. 7.— Polarisation as a function of solar zenith angle. Curves 1 and 2 are calculated for singly scattered light (P_S) in a clear atmosphere, curves 3 and 4 are averaged measurements of the total polarisation (P), and curves 5 and 6 are the calculated polarisation for multiply scattered light (P_M). The dashed lines are for polarisation at 480 nm and the solid lines are for 690 nm . (Plot is from Pavlov et al. (1995)).

in each regime. P also behaves somewhat differently for red and blue wavelengths, with a division around $\lambda = 550 \text{ nm}$. Note that $P(Z_\odot)$ usually shows day to day variations at each site and there is some overlap in the 3 ranges of solar zenith angle. This is probably caused by different weather conditions and vertical aerosol concentrations.

The typical behaviour of the degree of polarisation P as a function of Z_\odot and λ is summarised in Table 5, which is derived from the work of Bondarenko (1964), Coulson (1980), Pavlov et al. (1995), Ougolnikov & Maslov (2003) and Postlyakov et al. (2003). Figure 7, from Pavlov et al. (1995), shows the typical variations of single, multiple and total polarisation as a function of solar zenith angle during twilight.

The $Z_\odot = 102 - 108^\circ$ regime is where one might have hoped to turn twilight into dark time. However, as shown in Table 5, measurements at other sites show the polarisation in this range to be less

TABLE 5
TYPICAL BEHAVIOUR OF THE DEGREE OF POLARISATION WITH Z_{\odot} AND λ .

	$Z_{\odot} = 90 - 96^{\circ}$	$Z_{\odot} = 96 - 102^{\circ}$	$Z_{\odot} = 102 - 108^{\circ}$
P (blue λ)	Maximum: $Z_{\odot}=92 - 94^{\circ}$ Decreases with increasing Z_{\odot} λ dependent	Steep decrease with increasing Z_{\odot} then a flat or a minimum section between 98 & 102°	Steep decrease with increasing Z_{\odot} then starts to flatten at $Z_{\odot} \sim 104^{\circ}$
P (red λ)	Maximum: $Z_{\odot} = 90^{\circ}$ Decreases with increasing Z_{\odot} λ independent	Steady decrease Occasional 2 nd maximum associated with aerosols	Steep decrease
Processes	I_S dominates over I_M I_N negligible	I_M dominates over I_S I_N negligible for $Z_{\odot} < 98^{\circ}$ $P < 60\%$ for both ranges	I_S dominates over I_M for $Z_{\odot} > 104^{\circ}$ I_N dominates over I_S and I_M P strongly λ dependent Aerosol scattering important $P < 50\%$ for both ranges
Polariser advantage	$Z \sim 90^{\circ}, I_O > 5.3$ $Z \sim 92^{\circ}, I_O > 5.7$ $Z \sim 94^{\circ}, I_O > 7.2$ $Z \sim 96^{\circ}, I_O > 9.9$	$Z \sim 98^{\circ}, I_O > 14.3$ $Z \sim 100^{\circ}, I_O > 18.3$	No advantage in using a polariser

References. — Bondarenko (1964), (Coulson 1980), (Coulson 1988), Pavlov et al. (1995)

NOTE.—The last row shows the maximum object brightness, I_O , in mag arcsec⁻² for which a polariser will yield an advantage at 690 nm, based on the results of (Pavlov et al. 1995).

than about 50%, and hence, as discussed in Section 4.2, the use of a polariser would not be beneficial. The total polarisation at Dome C at these solar zenith angles is likely to be similar to the sites discussed because all measurements were taken at clean high altitude sites (therefore with small Rayleigh optical depths) on visibly clear days. We therefore conclude that there is likely to be no gain in using a polariser, in this regime.

For observations of bright stars (for example, direct imaging of exoplanets around host stars of typical magnitudes $V = 11$) a high sky background can be tolerated. Using a polariser for this type of observation could be advantageous during those times when the sun is up to 6 degrees below the horizon.

5. Conclusions

Dome C has a comparable number of cloud-free, astronomically dark hours to a more temperate site such as Mauna Kea. Nevertheless, the fraction of sky observable at Dome C is considerably lower than at Mauna Kea. Atmospheric scattering at Dome C should be close to the lowest anywhere on Earth, reducing the sky brightness contributions from sunlight, moonlight and tropospheric scattering, and reducing the extinction throughout the optical. The moonlight contribution to sky brightness over the year is less than at lower latitude sites. Aurorae will rarely be more than 7° above the horizon and will typically be more than about 1160 km away; they will generally be unobservable. Zodiacal light is darker at the zenith and 60° from zenith than at equatorial sites and will always be darker in V than $23.1 \text{ mag arcsec}^{-2}$ at zenith. Airglow is essentially the same at all sites. The integrated starlight and diffuse galactic light will be slightly brighter at Dome C than at other sites because the galactic plane is always close to zenith. There is no artificial light pollution at Dome C; a condition that should persist indefinitely.

In early evening twilight and late morning twilight, some advantage could be gained through the use of polarising filters. However, as the sky becomes darker, such filters are of less benefit.

Dome C thus appears to be an attractive site for optical as well as infrared astronomy. Versatile facilities such as the proposed two metre telescope

PILOT (Pathfinder for an International Large Optical Telescope (Burton et al. 2005)) should therefore be able to achieve their scientific potential at Dome C across the full observable spectrum.

This research is supported by the Australian Research Council. SLK is supported by an Australian Postgraduate Award and by an Australian Antarctic Division top-up scholarship. The authors would like to thank Anna Moore for helpful discussions and Eric Aristidi for permission to quote the results of the University of Nice group prior to publication. We would especially like to thank Gary Burns for very helpful comments on an earlier draft, and the referee, Ferdinando Patat, for his useful suggestions which have significantly improved the paper.

REFERENCES

- Agabi, A., et al. 2005, PASP, in press
- Anderson, D.E. & Lloyd, S.A. 1990, *J. Geophys. Res.*, 95, 7429
- Aristidi, E., et al. 2005a, *A&A*, 430, 739
- Aristidi, E., et al. 2005b, *A&A*, in press
- Aristidi, E., et al. 2005c, *Acta Astron. Sinica Supp.*, in press
- Ashley, M.C.B., Burton, M.G., Calisse, P.G., Phillips, A. & Storey, J.W.V. 2005, *Highlights of Astronomy*, ASP Conference Series, 13, 936
- Baldry, I.K. & Bland-Hawthorn, J. 2001, *MNRAS*, 322, 201
- Benn, C.R. & Ellison, S.L. 1998, La Palma Technical Note 115 (Issac Newton Group, La Palma)
- Bodhaine, B.A. 1995, *J. Geophys. Res.*, 100, 8967
- Bodhaine, B.A., Wood, N.B., Dutton, E.G. & Slusser J.R. 1999, *J. Atmos. Ocean. Tech.*, 16, 1854
- Bondarenko, L.N. 1964, *Soviet Ast.*, 8, 299
- Burns, G.B., French, W.J.R., Greet, P.A., Phillips, F.A., Williams, P.F.B., Finlayson, K., & Klich, G. 2002, *J. Atmos. Terr. Phys.*, 64, 1167

- Burton, M.G., et al. 2005, PASA, 22, 199
- Calisse, P.G., Ashley, M.C.B., Burton, M.G., Phillips, M.A., Storey, J.W.V., Radford, S.J.E. & Peterson, J.B. 2004, PASA, 21, 256
- Candidi, M. & Lori, A. 2003, Mem. Soc. Astron. Italiana, 74, 29
- Cinzano, P. & Elvidge, C.D. 2001, MNRAS, 328, 689
- Cinzano, P. & Elvidge, C.D. 2004, MNRAS, 353, 1107
- Collins, R.L., Bowman, K.P. & Gardner, C.S. 1993, J. Geophys. Res., 98, 1001
- Coulson, K.L. 1980, Appl. Opt., 19, 3469
- Coulson, K.L. 1998, *Polarization and intensity of light in the atmosphere*, (Hampton, Virginia USA, A. Deepak Publishing)
- Deeg, H.J., Belmonte, J.A., Alonso, R., Horne, K., Alsubai, K. & Doyle, L.R. 2005, EAS Publications Series, 14, 303
- Dempsey, J.T., Storey, J.W.V. & Phillips, A. 2005, PASA, 22, 91
- Fitch, B.W. & Coulson, K.L. 1983, Appl. Opt., 22, 71
- Garcia, R.R & Soloman, S. 1985, J. Geophys. Res., 90, 3850
- Garstang, R.H. 1989, PASP, 101, 306
- Garstang, R.H. 1989, ARA&A, 27, 19
- Krisciunas, K. & Schaefer, B.E. 1991, PASP, 103, 1033
- Lawrence, J.S. 2004, PASP, 116, 482
- Lawrence, J.S., Ashley, M.C.B., Tokovinin, A. & Travouillon, T. 2004, Nature, 431, 278
- Leinert, C., et al. 1998, A&AS, 127, 1
- Le Texier, H., Soloman, S. & Garcia R.R. 1987, Planet. Space Sci., 35, 977
- NGDC, National Geophysical Data Center, 2005, *Estimated Values of Magnetic Field Properties*, <http://www.ngdc.noaa.gov/ngdc.html>
- Ortolani, S. (editor) 2003, ESPAS Site Summary Series: Mauna Kea, Issue 1.2, Section 3
- Ougolnikov, O.S. 1999, Cosmic Research, 37, 168
- Ougolnikov, O. & Maslov, I. 2003, Proc. SPIE, 5026, 219
- OVATION 2005, The Auroral Particles and Imagery Group, The John Hopkins University, <http://sd-www.jhuapl.edu/Aurora/index.html>
- Patat, F. 2003, A&A, 400, 1183
- Patat, F. 2004, ESO Messenger, 118, 11
- Pavlov, V.E., Egorova, L.A., Kardopolov, V.I., Rspaev, F.K. & Ukhinov, S.A. 1995, Atm. Oce. Phys., 30, 449
- Phillips, A., Burton, M.G., Ashley, M.C.B., Storey, J.W.V., Lloyd, J.P., Harper, D.A., & Bally, J. 1999, ApJ, 527, 1009
- Pomozi, I., Horvath, G. & Wehner, R. 2001, J. Exp. Bio, 204, 2933
- Postylyakov, O.V., Ugolnikov, O.S., Maslov, I.A. & Sidorchuk, A.A 2003, EGS-AGU-EUG Joint Assembly, Abstracts from the meeting held in Nice, France, 6 - 11 April 2003, abstract #13842, 13842
- Rayleigh, L. 1928, Proc. Roy. Soc. London, Ser. A., 119, 11
- Roach, F.E & Gordon, J.L. 1973, *The light of the night sky*, (Dordrecht, Holland, D.Reidel Publishing Company)
- Rozenberg, G.V. 1966, *Twilight, A Study in Atmospheric Optics*, Plenum Press, New York
- Shepherd, G.G., Roble, R.G., McLandress, C. & Ward, W.E. 1997, J. Atmos. Solar-Terr. Phys., 59, 655
- Sivjee, G.G., S.M.I. Azeem & B. A. Emery, 12 Sep 2005: South Pole Michelson Interferometer, <http://cedarweb.hao.ucar.edu>
- Storey, J.W.V., Ashley, M.C.B., Lawrence, J.S. & Burton, M.G. 2003, Mem. Soc. Astron. Italiana Supp., 2, 13
- Storey, J.W.V., Ashley, M.C.B., Burton, M.G. & Lawrence, J.S. 2005, EAS Pub. Ser., 14, 7

- Tomasi, C., Vitale, V., Petkov, B., Lupi, A. & Cacciari, A. 2005, *Appl. Opt.*, 44, 3320
- Ugolnikov, O.S., Postylyakov, O.V. & Maslov, I.A. 2004, *J. Quant. Spec. Radiat. Transf.*, 88, 233
- Valenziano, L. & dall'Oglio, G. 1999, *PASA*, 16, 167
- Walden, V.P., Town, M.S., Halter, B. & Storey, J.W.V. 2005, *PASP*, 117, 300
- Walker, M.F. 1988, *PASP*, 100, 496
- Yee, J.-H., Crowley, G., Roble, R.G., Skinner, W.R., Burrage, M.D. & Hays, P.B. 1997, *J. Geophys. Res.*, 102, 19949
- Zaragoza, G., Taylor, F.W. & López-Puertas, M. 2001, *J. Geophys. Res.*, 106, 8027
- Zuev, V. E. 1974 *Propagation of visible and infrared radiation in the atmosphere*, (Keter Publishing House Jerusalem, Translation from Russian of *Rasprostranenie vidimyykh i infrakrasnykh voln v atmosfere*. Translated by D.Lederman, translation edited by P.Greenberg)